Regioselectivity of the Addition of O₂ on SPS-Based Rhodium(I) and Iridium(I) Complexes

Marjolaine Doux, Louis Ricard, Pascal Le Floch,* and Yves Jean*

Laboratoire "Hétéroéléments et Coordination" UMR CNRS 7653, Ecole Polytechnique, 91128 Palaiseau Cedex, France

The addition of O₂ on SPS-type pincer-based Rh(I) and Ir(I) complexes was studied by means of DFT calculations. The regioselectivity and the influence of the nature of the metal center on the reaction thermicity were related through a thermodynamic cycle to the electronic properties of the metal complex and to the energetics of the M−O bonds. The synthesis and the X-ray crystal structure analysis of the Ir(I) complex are also presented.

Introduction

Polydentate ligands featuring different heteroatoms as binding sites are currently attracting great attention both in coordination chemistry and in catalysis.[1] Indeed, it is now well recognized that the combination of very different electronic and steric effects can lead to subtle changes in the coordinating behavior of ligands as well as the reactivity of their respective complexes. Modulation of these electronic effects were found to play an important role in many catalytic processes.[2] Among different possible combinations only little attention has been paid to mixed P−S ligands, probably because of the reputation of sulfur to act as a poison for catalysis.[3] However, some P−S-based catalytic systems, even operating at high temperature with low-valent metals, already proved to be efficient catalysts.[4] Recently, we

reported on the synthesis,[5] the coordination chemistry,[6] and the use in catalysis[7] of a new type of SPS pincer ligand featuring two P=S groups as ancillary ligands and a central phosphorus atom as binding site. The anionic tridentate ligands, which are easily assembled from the corresponding phosphinines through a nucleophilic attack on phosphorus, were found to strongly activate 16e Rh(I) centers. Thus, a neutral Rh(I) complex, [Rh(SPS)(PPh₃)] (**4**), reacted with O₂ and CS₂ to yield the corresponding pseudo-octahedral η²-Rh(III) complexes **5**, which are depicted in Scheme 1.[8] Surprisingly, all these reactions proceeded with complete regioselectivity, the attack taking place on the *syn* face (to the substituent at phosphorus) of the square-planar complex. This unusual facial discrimination had not been rationalized before, and in this paper we present the results of a DFT study that shed some light on this surprising reactivity. Additional experiments and calculations regarding the reactivity of the Ir complexes **6**−**9** are also reported.

Results and Discussion

The ability of the SPS-type pincer-based Rh(I) and Ir(1) complexes to activate the O₂ molecule was studied by means of DFT calculations, using model complexes (noted as [M(SPS)(PH₃)] with M = Rh, Ir) in which the phenyl groups were replaced by H atoms. Four modes of attack were considered (*syn*-SS, *anti*-SS, *syn*-PP, and *anti*-PP) depending whether the incoming O₂ molecule is located (i) *syn* or *anti* to the P−Me bond and (ii) coplanar to the M−S bonds (SS) or to the M−P bonds (PP) (Scheme 2). The regioselectivity of the addition reaction as well as the influence of the nature of the metal center on its thermicity were related through a thermodynamic cycle to the electronic properties of the metal complex and to the energetics of the M−O bonding.

* To whom correspondence should be addressed. Tel: +33.1.69.33.45.70. Fax: +33.1.69.33.39.90. E-mail: lefloch@poly.polytechnique.fr, yves.jean@polytechnique.fr.
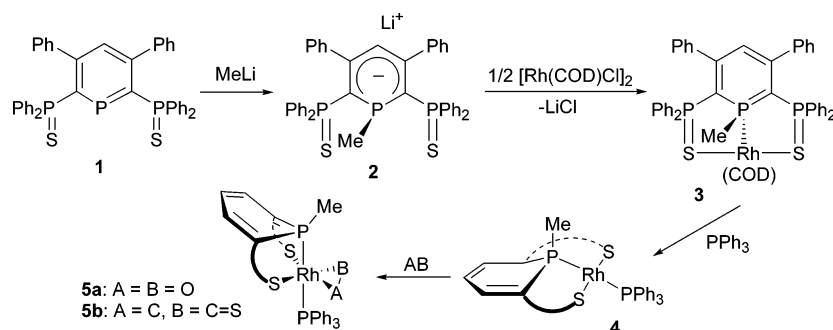
(1) (a) Bader, A.; Lindner, E. *Coord. Chem. Rev.* **1991**, *108*, 27. (b) Hovestad, N. J.; Eggeling, E. B.; Heidbüchel, H. J.; Jastrzebski, J. T. B. H.; Kragl, U.; Keim, W.; Vogt, D.; van Koten, G. *Angew. Chem., Int. Ed.* **1999**, *38*, 1655. (c) Weber, R.; Englert, U.; Ganter, B.; Keim, W.; Möthrath, M. *Chem. Commun.* **2000**, 1419. (d) Braunstein, P.; Naud, F.; Rettig, S. *New J. Chem.* **2001**, *25*. (e) Albrecht, M.; Van Koten, G. *Angew. Chem.* **2001**, *113*, 3866. (f) Dai, W.-M.; Yeung, K. K. Y.; Liu, J.-T.; Zhang, Y.; Williams, I. D. *Org. Lett.* **2002**, *4*, 1615. (g) Andrieu, J.; Richard, P.; Camus, J.-M.; Poli, P. *Inorg. Chem.* **2002**, *41*, 3876. (h) Thoumazet, C.; Melaimi, M.; Ricard, L.; Mathey, F.; Le Floch, P. *Organometallics* **2003**, *22*, 1580. (i) Agbossou-Niedercorn, F.; Suisse, I. *Coord. Chem. Rev.* **2003**, *242*, 145. (j) van der Boom, M. E.; Milstein, D. *Chem. Rev.* **2003**, *103*, 1759. (k) Barloy, L.; Malaisé, G.; Ramdeehul, S.; Newton, C.; Osborn, J. A.; N., K. *Inorg. Chem.* **2003**, *42*. (l) Bunlaksananusorn, T.; Polborn, K.; Knochel, P. *Angew. Chem., Int. Ed.* **2003**, *42*. (m) Franco, D.; Gómez, M.; Jiménez, F.; Muller, G.; Rocamora, M.; Maestro, M. A.; Mahía, J. *Organometallics* **2004**, *23*, 3177. (n) Maire, P.; Deblon, S.; Breher, F.; Geier, G.; Böhler, C.; Rüegger, H.; Schönberg, H.; Grützmacher, H. *Chem. Eur. J.* **2004**, *10*, 4198.

(2) See for example: Braunstein, P.; Naud, F. *Angew. Chem., Int. Ed.* **2001**, *40*, 680.

(3) (a) Bayón, J. C.; Claver, C.; Masdeu-Bultó, A. M. *Coord. Chem. Rev.* **1999**, *193−195*, 73. (b) Mizuta, T.; Imamura, Y.; Miyoshi, K. *J. Am. Chem. Soc.* **2003**, *125*, 2068. (c) Kostas, I. D.; Steele, B. R.; Andreadaki, F. J.; Potapov, V. A. *Inorg. Chim. Acta* **2004**, *357*, 2850.

(4) (a) Baker, M. J.; Giles, M. F.; Orpen, A. G.; Taylor, M. J.; Watt, R. J. *Chem. Commun.* **1995**, 197. (b) Suranna, G. P.; Mastrorilli, P.; Nobile, C. F.; Keim, W. *Inorg. Chim. Acta* **2000**, *305*, 151. (c) Gonsalvi, L.; Adams, H.; Sunley, G. J.; Ditzel, E.; Haynes, A. *J. Am. Chem. Soc.* **2002**, *124*, 13597. (d) Liang, H.; K., N.; Ito, S.; Yoshifuji, M. *Tetrahedron Lett.* **2003**, *44*, 8297. (e) Ito, S.; Liang, H.; Yoshifuji, M. *Chem. Commun.* **2003**, 398.

(5) Doux, M.; Bouet, C.; Mézailles, N.; Ricard, L.; Le Floch, P. *Organometallics* **2002**, *21*, 2785.

(6) Doux, M.; Mézailles, N.; Ricard, L.; Le Floch, P. *Eur. J. Inorg. Chem.* **2003**, 3878.

(7) Doux, M.; Mézailles, N.; Melaimi, M.; Ricard, L.; Le Floch, P. *Chem. Commun.* **2002**, 1566.

(8) Doux, M.; Mézailles, N.; Ricard, L.; Le Floch, P. *Organometallics* **2003**, *22*, 4624.
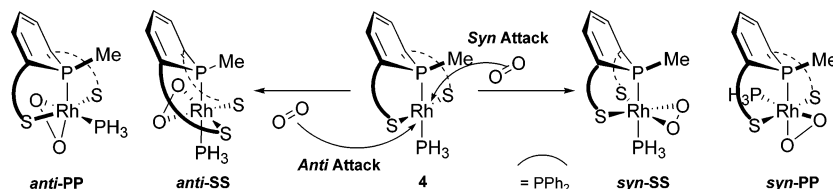
Scheme 1

Scheme 2

Table 1. Main Geometrical Parameters Optimized for the [M(SPS)(PH₃)] Complex for M = Rh, Ir (see Figure 1 for the atom numbering)[a]

[M(SPS)PH₃]	M = Rh	M = Ir
M−P1	2.259 (2.243)	2.274
M−P4	2.303 (2.303)	2.272
M−S1	2.401 (2.320)	2.380
M−S2	2.401 (2.321)	2.380
P1−Me	1.839 (1.820)	1.837
P1−C2	1.799 (1.794)	1.797
P1−C6	1.799 (1.805)	1.797
P2−C2	1.762 (1.763)	1.763
P3−C6	1.762 (1.769)	1.763
P2−S1	2.030 (2.024)	2.041
P3−S2	2.030 (2.022)	2.041
C2−P1−C6	99.8 (101.4)	100.1
Σ (C−P1−C)	311.0 (311.2)	312.6
S1−M−S2	173.9 (172.5)	172.7
P1−M−P4	174.3 (174.7)	171.4
P1−C2−P2	111.9 (113.6)	111.7
P1−C6−P3	111.9 (111.1)	111.6
C2−P2−S1	111.9 (109.8)	111.4
C6−P3−S2	111.9 (109.6)	111.4
M−S1−P2	99.4 (107.7)	97.9
M−S2−P3	99.4 (101.3)	97.9

[a] Bond lengths are in Å and angles in deg. Experimental values are given in parenthesis for the Rh complex.[8]
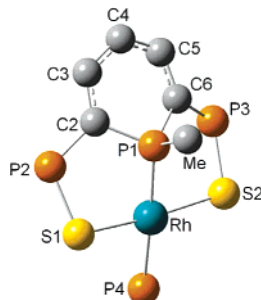

Figure 1. Optimized geometry of ¹[Rh(SPS)(PH₃)]. Hydrogen atoms are omitted for clarity.

In a first set of calculations, the geometry of the complex [Rh(SPS)(PH₃)] was optimized in its lowest singlet state without any symmetry constraint. The main theoretical parameters are reported in the first column of Table 1 together with the experimental values. A nearly square-planar arrangement was found around the Rh center with P1−Rh−P4 and S1−Rh−S2 angles of 174.3° and 173.9°, respectively (exptl 174.7° and 172.5°, respectively). There is an excellent agreement between the experimental and theoretical bond lengths (deviations smaller than 0.020 Å) with the exception of the Rh−S distance, which is overestimated by 0.080 Å (Figure 1).[9]

The geometry of the addition complex [(Rh(SPS)(PH₃)-(O₂)] was studied for the *syn*-SS, *syn*-PP, *anti*-PP, and *anti*-SS attacks of O₂ (Scheme 2). Four different isomers (**Ia−IVa**) were actually optimized and further characterized as minima on the potential energy surface. Their structures are depicted in Figure 2 together with selected geometrical parameters (see also the Supporting Information). A pseudo-octahedral complex featuring an η^2 coordination of O₂ was found for three first approaches (**Ia−IIIa**). On the other hand, the *anti*-SS attack led to the breaking of a metal−sulfur bond and the formation of a complex with a distorted trigonal bipyramid geometry (**IVa**), the oxygen atoms of the η^2-O₂ molecule occupying two equatorial sites.[10] In agreement with the experimental data, the *syn*-SS isomer was found to be the most stable isomer, the energy ordering being (in kcal mol⁻¹) *syn*-SS (**Ia**) (0) < *anti*-PP (**IIa**) (+7.1) < *anti*-SS (**IVa**) (+11.7) < *syn*-PP (**IIIa**) (+13.7). The energy differences are large enough to understand why only the *syn*-SS isomer (**Ia**) has been observed experimentally. Furthermore, it is the only isomer that was found to be more stable than the isolated reactants ($\Delta E_R = -5.1$ kcal mol⁻¹). The O−O distance, elongated from 1.208 Å in free O₂ to 1.386 Å (exptl 1.431(2) Å), and the Rh−O distances of 2.021 and 2.023 Å (exptl $(2.027(2))_{av}$ Å) are consistent with a Rhᴵᴵᴵ peroxo struc-

(9) The discrepancy between the experimental and theoretical structure was slightly reduced when the phenyl substituents on the phosphorus centers and as well as on the phosphinine ring were taken into account by means of QM/MM calculation (see computational details and Supporting Information). The optimized Rh−S distance (2.388 Å) is 0.067 Å longer than the experimental value.

(10) A pseudo-octahedral structure associated with the *anti*-SS attack on the Rh complex was also characterized as a minimum on the potential energy surface. However its energy is located 9.7 kcal mol⁻¹ above that of **IVa**. The same holds for the *anti*-SS attack on the Ir complex, the energy of the pseudo-octahedral structure being found to be 17.7 kcal mol⁻¹ above that of **IVb**.
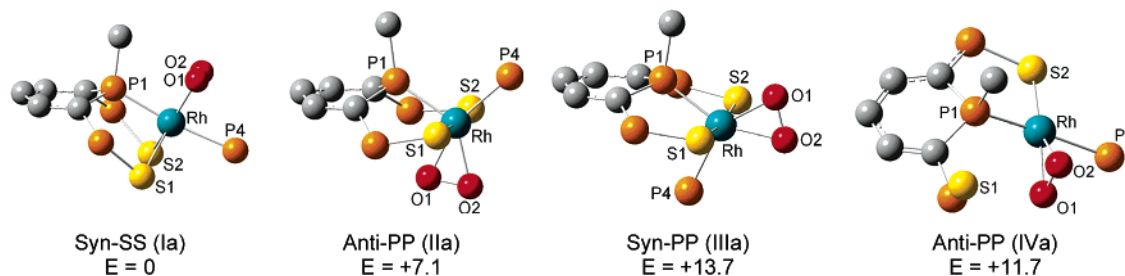
Figure 2. Optimized geometries of rhodium complexes **Ia−IVa**. Hydrogen atoms are omitted for clarity. E: relative energy in kcal mol⁻¹. Selected geometrical parameters (in Å and deg). **Ia**: O1−O2 1.386, Rh−O1 2.021, Rh−O2 2.023, Rh−S1 2.494, Rh−S2 2.500, Rh−P1 2.297, Rh−P4 2.358, S1−Rh−S2 93.2, P1−Rh−P4 173.4. **IIa**: O1−O2 1.384, Rh−O1 1.989, Rh−O2 2.062, Rh−S1 2.420, Rh−S2 2.4420, Rh−P1 2.307, Rh−P4 2.321, S1−Rh−S2 177.7, P1−Rh−P4 104.6. **IIIa**: O1−O2 1.380, Rh−O1 2.005, Rh−O2 2.061, Rh−S1 2.425, Rh−S2 2.426, Rh−P1 2.265, Rh−P4 2.345, S1−Rh−S2 171.5, P1−Rh−P4 101.5. **IVa**: O1−O2 1.359, Rh−O1 2.003, Rh−O2 1.999, Rh−S1 5.601, Rh−S2 2.328, Rh−P1 2.327, Rh−P4 2.400, S2−Rh−O1 161.3, S2−Rh−O2 158.2, P1−Rh−P4 175.1.

Scheme 3
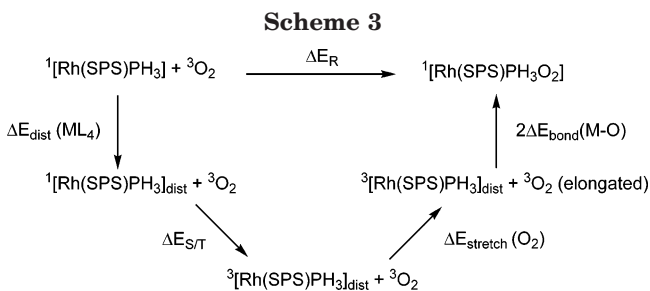
ture (Figure 2, **Ia**). The bond angles in the plane defined by the two sulfur ligands and the oxygen molecule are satisfactorily reproduced: S1−Rh−S2 = 93.2° (exptl 98.7°) and O1−Rh−O2 = 40.1° (exptl 41.3°).

The electronic factors responsible for the regioselectivity of this oxidative addition reaction can be analyzed by means of a thermodynamic cycle which connects the separate reactants (^{1}[Rh(SPS)(PH$_3$)] + ^{3}O$_2$) to the peroxo complex (**Ia−IVa**) (Scheme 3). The reaction is decomposed into the following steps: (i) distortion of the ^{1}[Rh(SPS)(PH$_3$)] complex from its equilibrium geometry to its geometry in the product (ΔE_{dist}(ML$_4$)); (ii) formation of the triplet state ($\Delta E_{S/T}$); the distorted metal fragment with two unpaired electrons is now in the optimal situation to form two new bonds; (iii) stretching of O$_2$ to its actual bond distance in the product ($\Delta E_{stretch}$(O$_2$)); (iv) formation of the M−O bonds ($2\Delta E_{bond}$(M−O)). The energy change associated with the addition reaction (ΔE_R) can thus be expressed as $\Delta E_R = \Delta E_{dist}$(ML$_4$) + $\Delta E_{S/T} + \Delta E_{stretch}$(O$_2$) + $2\Delta E_{bond}$(M−O). In the following discussion, the two first terms will be most often considered together since their sum (quoted as $\Sigma = \Delta E_{T\ dist}$) represents the energy required to "prepare" the metal fragment for the oxidative addition reaction.

Results of this energy decomposition are given in Table 2a. Both the triplet state energy of the distorted metal fragment and the energies of the bonds under formation come out to be important factors to rationalize the selectivity observed experimentally. It is noteworthy that the *syn*-SS isomer (**Ia**) is favored with respect to the other isomers by the smallest triplet metal fragment energy ($\Delta E_{T\ dist}$) and by the strongest Rh−O bonding energy. For instance, if one compares the two most stable isomers, *syn*-SS (**Ia**) and *anti*-PP (**IIa**), both $\Delta E_{T\ dist}$(Rh−O) (by 4.7 kcal mol⁻¹) and $2\Delta E_{bond}$(Rh−O) (by 2.8 kcal mol⁻¹) terms work in favor of the experimentally observed *syn*-SS isomer.

Table 2. Energy Decomposition (kcal mol⁻¹) for the Formation of I−IV Isomers by the Addition of O₂ on the [M(SPS)(PH₃)] Complex: (a) M = Rh; (b) M = Ir

(a)				
M = Rh	*syn*-SS (**Ia**)	*anti*-PP (**IIa**)	*syn*-PP (**IIIa**)	*anti*-SS (**IVa**)
ΔE_{dist}(ML$_4$)	+27.1	+31.2	+35.3	+31.9
$\Delta E_{S/T}$	−1.4	−0.8	−1.9	+4.9
$\Sigma = \Delta E_{T\ dist}{}^a$	+25.7	+30.4	+33.4	+36.8
$\Delta E_{strech}{}^3$(O$_2$)	+20.6	+20.2	+19.4	+15.6
$2\Delta E_{bond}$(M−O)	−51.4	−48.6	−44.2	−45.8
$\Delta E_R{}^b$	−5.1	+2.0	+8.6	+6.6

(b)				
M = Ir	*syn*-SS (**Ib**)	*anti*-PP (**IIb**)	*syn*-PP (**IIIb**)	*anti*-SS (**IVb**)
ΔE_{dist}(ML$_4$)	+36.9	+39.1	+48.1	+41.2
$\Delta E_{S/T}$	−6.3	−2.3	−5.7	−0.6
$\Sigma = \Delta E_{T\ dist}{}^a$	+30.6	+36.8	+42.4	+40.6
$\Delta E_{strech}{}^3$(O$_2$)	+26.8	+27.4	+27.3	+20.4
$2\Delta E_{bond}$(M−O)	−73.4	−77.7	−74.2	−63.7
$\Delta E_R{}^b$	−16.0	−13.5	−4.5	−2.7

$^a \Sigma = \Delta E_{T\ dist} = \Delta E_{dist}$(ML$_4$) + $\Delta E_{S/T}$. $^b \Delta E_R = \Delta E_{dist}$(ML$_4$) + $\Delta E_{S/T} + \Delta E_{strech}{}^3$(O$_2$) + $2\Delta E_{bond}$(M−O).

Similar calculations were performed on the Ir analogue. The *syn*-SS isomer (**Ib**) was still found to be the most stable isomer, the energy ordering being (in kcal mol⁻¹) *syn*-SS (**Ib**) (0) < *anti*-PP (**IIb**) (+2.5) < *syn*-PP (**IIIb**) (+11.5) < *anti*-SS (**IVb**) (+13.3). The energy decomposition shows that this result can be mainly traced to triplet state energy of the distorted metal fragment ($\Delta E_{T\ dist}$, Table 2b). As a matter of fact, this term parallels the relative energies of the three most stable isomers, whereas the Ir−O bonding energy favors an addition *trans* to the Ir−P bonds (*anti*-PP and *syn*-PP isomers). As it has been shown previously,[11] the $\Delta E_{T\ dist}$ term comes out to be an important factor to predict the outcome of an oxidative addition reaction. The energy difference between the two most stable isomers (*syn*-SS and the *anti*-PP) is rather small (2.5 kcal mol⁻¹) since the Ir−O bonding energy and the $\Delta E_{T\ dist}$ terms work in opposite directions. From a structural point of view, the O−O and Ir−O distances optimized in the *syn*-SS isomer (**Ib**) were found to be equal to 1.418 Å and 2.025 Å, respectively, a result consistent with an Ir^{III}

(11) (a) Su, M.-D.; Chu, S.-Y. *J. Am. Chem. Soc.* **1997**, *119*, 5373. (b) Tomas, J.; Lledos, A.; Jean, Y. *Organometallics* **1998**, *17*, 4932. (c) Lesnard, H.; Demachy, I.; Jean, Y.; Lledos, A. *Chem. Commun.* **2003**, 850.
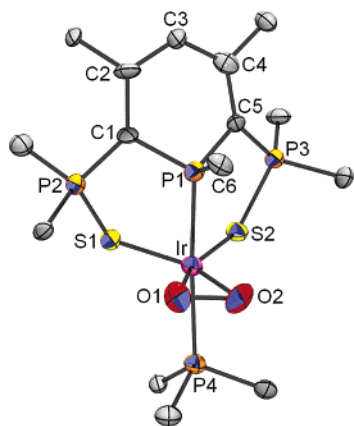
Figure 3. ORTEP view of complex **9**. Phenyl groups have been omitted for clarity. Ellipsoids are scaled to enclose 50% of the electron density. The numbering is arbitrary and different from that used in the assignment of NMR spectra. Relevant distances (Å) and bond angles (deg): O1–Ir 2.01(1), O2–Ir 2.03(1), P1–Ir 2.263(4), P4–Ir 2.337(4), S1–Ir 2.405(5), S2–Ir 2.397(4), O1–O2 1.46(2), P1–C1 1.78(2), C1–C2 1.43(2), C2–C3 1.40(2), C3–C4 1.41(3), C4–C5 1.39(2), C5–P1 1.79(2), C1–P2 1.74(2), C5– P3 1.75(2), P2–S1 2.030(6), P3–S2 2.033(6), P1–Ir–P4 172.4-(2), S1–Ir–O1 113.3(4), O1–Ir–O2 42.5(5), O2–Ir–S2 118.7(4), C1–P1–C5 100.8(7).

peroxo structure (see also Supporting Information and experimental X-ray structure given in Figure 3).

The larger exothermicity of the addition reaction (-16.0 instead of -5.1 kcal mol^{-1}, Table 2) as well as the increase of the O–O distance in the most stable *syn*-SS isomer (from 1.386 in **Ia** to 1.418 Å in **Ib**) suggest that the activation of O₂ increases on going from Rh to Ir. The use of the thermodynamic cycle described in Scheme 3 offers a clear rationalization of this result. Comparison of the energy decomposition for the Rh (**Ia**) and Ir (**Ib**) *syn*-SS isomers (Table 2) shows that the evolution of the $\Delta E_{\text{T dist}}$ term is opposite that of ΔE_R, so that, taken alone, it would favor the reaction of the Rh complex. The only factor that makes the reaction with the Ir complex more exothermic is the M–O bonding energy, which is found to be much larger for M = Ir (-73.4 kcal mol^{-1}) than for M = Rh (-51.4 kcal mol^{-1}). This result examplifies the second important factor to rationalize the behavior of a complex in an oxidative addition reaction, i.e., the strength of the metal–ligand bonds under formation.

With these results at hand, we were stimulated to synthesize the iridium analogue of the rhodium complex **4** and to test its reactivity toward oxygen. A synthetic procedure analogous to the one used for the synthesis of **4** was followed (Scheme 1).

Complex **6** was easily prepared from the reaction of anion **2** with half an equivalent of the [Ir(COD)Cl]₂ precursor (Scheme 4). Complex **6**, which was isolated as a very stable orange solid, was fully characterized by NMR techniques and elemental analyses. Unfortunately, despite many attempts, **6** could not be crystallized and information about the spatial arrangement of the SPS ligand could not be obtained. Although ³¹P NMR spectroscopy revealed that the PPh₂S groups are magnetically equivalent, two geometries can be proposed for **6**: one in which the ligand is located in the plane and a second in which it caps one face of the

bipyramid (Scheme 4). In **6**, the ³¹P NMR signals of the SPS moiety appear as expected sets of a triplet and doublet at 7.9 ppm (P-Me) and 47.8 ppm (PPh₂S), respectively, with a ^2J(P–P) coupling constant of 112.4 Hz. Compared to its rhodium analogue, in **6** the chemical shift of the P-Me moiety is shifted toward high field ($\Delta\delta = -25.2$ ppm). The other important difference issues from the spin system pattern of the vinylic CH (COD) in the ¹³C NMR spectrum. Indeed, in **6**, these signals appear as a doublet at 62.0 ppm (^2J(C–P) = 6.3 Hz), whereas, in **3**, they appear as a broad singlet at 78.6 ppm. This could be explained by a better back-bonding of the metal into the alkene bond in the case of the iridium complex **6**. Apart from these data, these iridium and rhodium complexes did not differ to a great extent.

The displacement of the COD ligand in **6** by triphenylphosphine was attempted. Unfortunately, despite many efforts (temperature up to 80 °C, presence of H₂ up to 20 atm, reaction carried out in THF and in MeOH, use of PMe₃), no reaction occurred. Therefore, we turned our attention to the [Ir(COE)₂Cl]₂ precursor (COE = cyclooctene) in which the COE ligand was supposed to be more labile than the COD ligand. Following the same procedure, the iridium(I) complex **8** was readily synthesized from the reaction of anion **2** with half an equivalent of the [Ir(COE)₂Cl]₂ precursor (Scheme 5). Unfortunately, complex **8** was found to be not stable enough to be isolated and decomposed within 30 min in solution. Complex **8** was only characterized on the basis of its ³¹P NMR spectrum, in which the signals of the SPS moiety appeared as sets of a triplet and doublet at 13.9 ppm (P-Me) and 33.6 ppm (PPh₂S), respectively, with a ^2J(P–P) coupling constant of 114.2 Hz. Note that **7** can also be synthesized from the reaction of half an equivalent of [Ir(COE)₂Cl]₂ with a solution of anion **2** followed by reaction with triphenylphosphine. The solution immediately turned from red (anion **2**) to dark brown. After 1 h, the formation of complex **7** was completed. However, complex **7** proved to be highly reactive (vide supra). Any attempts of purification (drying or precipitation) caused the decomposition of the product. Therefore, complex **7** was stored in a THF solution in the glovebox without any possible purification. Like **8**, complex **7** was characterized only by ³¹P NMR spectroscopy, which revealed that the PPh₂S groups are magnetically equivalent and that therefore the structure is symmetrical. This spectrum exhibits an AB₂C spin system pattern. As expected, the ³¹P NMR signals of the SPS moiety appear as sets of a doublet of triplets and doublet of doublets at 19.8 ppm (P$_A$-Me) and 37.7 ppm (Ph₂P$_B$=S), respectively, and the triphenylphosphine (P$_C$Ph₃) ligands appear as a doublet of triplets at 30.9 ppm with ^2J(P$_A$–P$_B$) = 128.1, ^2J(P$_A$–P$_C$) = 370.2, and ^3J(P$_B$–P$_C$) = 37.9 Hz.

Finally, reaction with O₂ was attempted. Coordination readily occurred in THF by bubbling O₂ (1 atm) into a solution of **7** at -78 °C to form complex **9** (Scheme 5). The solution became orange and a precipitate formed within 2 h. The geometry of **9** could not be unambiguously established on the sole basis of NMR data. However, it is clear that the structure of **9** remains symmetrical and ³¹P NMR signals of the PPh₂ and PPh₃ moieties are highly shifted from $\Delta\delta = +12.5$ ppm and -26.0 ppm, respectively. As expected, all signals appear
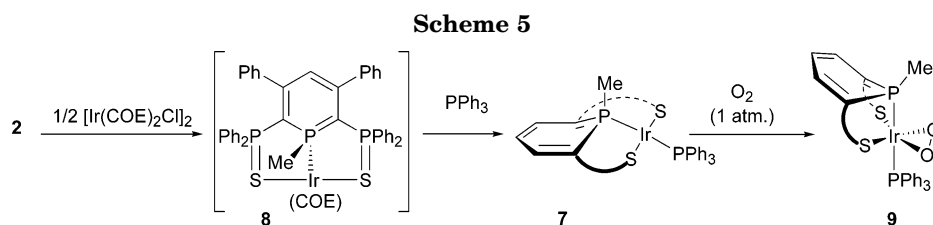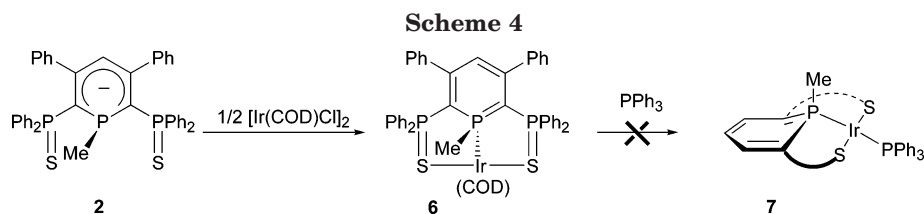
Scheme 4

Scheme 5

Table 3. Crystal Data and Structural Refinement Details for 9

formula	$C_{60}H_{49}IrO_2P_4S_2,C_4H_8O$
M_r	1254.30
cryst syst	monoclinic
space group	$P2_1/n$
a [Å]	16.891(2)
b [Å]	13.1160(10)
c [Å]	28.127(3)
β [deg]	106.870(10)
V [Å^3]	5963.2(11)
Z	4
ρ [g cm^{-3}]	1.397
μ [cm^{-1}]	2.460
cryst size [mm]	$0.14 \times 0.10 \times 0.03$
$F(000)$	2536
index ranges	$-19\ 19;\ -14\ 13;\ -31\ 31$
$2\theta_{max}$ [deg]/criterion	$23.82/I > 2\sigma I$
no. of params refined; data/param	669; 11
no. of reflns collected	16 433
no. of independ reflns	9044
no. of reflns used	7935
wR2	0.2296
R1	0.0767
goodness of fit	1.027
largest diff peak/hole [e Å^{-3}]	1.812(0.191)/$-3.036(0.191)$

as sets of doublets of triplets and doublets of doublets at 17.7 ppm (P$_A$-Me) and 50.2 ppm (P$_B$Ph$_2$S), respectively, and the triphenylphosphine (P$_C$Ph$_3$) as a doublet of triplets at 4.9 ppm with $^2J(P_A-P_B) = 100.1$, $^2J(P_A-P_C) = 428.5$, and $^3J(P_B-P_C) = 24.2.9$ Hz. Apart from this, the spectra of **9** do not deserve further comment.

Fortunately, small, twined crystals of complex **9** could be grown and analyzed by X-ray structure analysis. An ORTEP view of one molecule of **9** is presented in Figure 3 with the most significant metric parameters. Crystal data and structure refinement details are presented in Table 3. As predicted by DFT calculations, the overall geometry of complex **9** results from the *syn*-SS attack of O$_2$: the SPS ligand caps one face of the trigonal bipyramid. Examination of the O–O distance (1.46(2) Å) reveals that **9** is a Ir^{III} peroxo complex.[12] As can be seen by examining these data, there is an excellent fit between theoretical and experimental parameters. In **Ib** the SPS ligand, O–O, Ir–O, and Ir–P bond distances are very close to those of the X-ray structure of **9**: for instance, in **Ib** the P1–C1, C1–P2, P2–S1, O1–O2, Ir–O1, Ir–P1, and Ir–P4 are 1.793, 1.756, 2.032, 1.418,

(12) See for example: (a) Ho, D. G.; Ismail, R.; Franco, N.; Gao, R.; Leverich, E. P.; Tsyba, I.; Ho, N. N.; Baub, R.; Selke, M. *Chem. Commun.* **2002**, 570. (b) Teixidor, F.; Ayllon, J. A.; Vinas, C.; Sillanpaa, R.; Kivekas, R.; Casabo, J. *Inorg. Chem.* **1994**, *33*, 4815.

2.025, 2.302, 2.335 Å vs 1.78(2), 1.74(2), 2.030(6), 1.46-(2), 2.01(1), 2.263(4), 2.337(4) Å in **5a**. Moreover no discrepancies arise from the Ir–S distances: 2.468 in **Ib** vs 2.405(5) and 2.397(4) Å in **9**.

In conclusion, the regioselectivity of the addition of O$_2$ to the [Rh(SPS)(PH$_3$)] complex is well reproduced by DFT calculations. The *syn*-SS isomer is found to be favored by a factor related to a metal fragment property, i.e., the energy required to form the distorted complex in its lowest triplet state, and by the energetics of the Rh–O bonds under formation. Synthesis of the iridium analogue was also achieved and a *syn*-SS geometry is proposed on the basis of DFT calculations and confirmed by X-ray data. Finally, the increase of the exothermicity of the addition reaction on going from Rh to Ir is found to reflect the increase of the M–O bonding energy (Ir > Rh).

Experimental Section

General Considerations. All reactions were routinely performed under an inert atmosphere of argon or nitrogen by using Schlenk and glovebox techniques and dry deoxygenated solvents. Dry THF and hexanes were obtained by distillation from Na/benzophenone dry ether from CaCl$_2$ and then NaH and dry CH$_2$Cl$_2$ from P$_2$O$_5$. CDCl$_3$ was dried from P$_2$O$_5$ and stored on 4 Å Linde molecular sieves. CD$_2$Cl$_2$ was stored on 4 Å Linde molecular sieves in the glovebox. [Ir(COD)Cl]$_2$ was purchased from Strem chemicals and stored under nitrogen. Nuclear magnetic resonance spectra were recorded on a Bruker Advance 300 spectrometer operating at 300.0 MHz for ^{1}H, 75.5 MHz for ^{13}C, and 121.5 MHz for ^{31}P. Solvent peaks are used as internal reference relative to Me$_4$Si for ^{1}H and ^{13}C chemical shifts (ppm); ^{31}P chemical shifts are relative to a 85% H$_3$PO$_4$ external reference. Coupling constants are given in hertz. The following abbreviations are used: s, singlet; d, doublet; t, triplet; q, quadruplet; p, pentuplet; m, multiplet; v, virtual. Elemental analyses were performed by the "Service d'analyse du CNRS", at Gif sur Yvette, France. Phosphinine **1**,[5] anion **2**,[6] and [Ir(COE)$_2$Cl]$_2$ [13] were prepared according to reported procedures.

Synthesis of Complex 6. A solution of MeLi in Et$_2$O (95 μL, $C = 1.6$ M, 0.15 mmol) was syringed into a solution of **1** (100 mg, 0.15 mmol) in THF (5 mL) at -78 °C. The solution was warmed to room temperature and stirred for 20 min. Complete formation of **2** is checked by ^{31}P NMR (THF): δ 44.83 (d, $^2J(P-P) = 156.7$, PPh$_2$), -66.52 (t, $^2J(P-P) = 156.7$, PMe). In the glovebox, [Ir(COD)Cl]$_2$ (49.3 mg, 0.07 mmol) was added

(13) Herde, J. L.; Lambert, J. C.; Senoff, C. V.; Cushing, M. A. In *Inorganic Syntheses*; Parshall, G. W., Ed.; R. E. Krieger Publishing Company: Malabar, FL, 1982; Vol. 15, p 19.

and the solution was stirred for 30 min. After removing the solvent, the solid was washed first with hexanes (3 × 2 mL) then with ether (3 × 2 mL). The resulting solid was dissolved in CH_2Cl_2 and filtrated through Celite. After drying, **5** was recovered as an orange solid. Yield: 126 mg (86%). Anal. (%) calcd for $C_{50}H_{46}IrP_3S_2$: C 60.28, H 4.65. Found: C 59.92, H 4.17. ^{31}P ($CDCl_3$): δ 7.86 (t, $^2J(P_A-P_B) = 112.4$, P_AMe), 47.84 (d, $^2J(P_A-P_B) = 112.4$, P_BPh$_2$). ^1H ($CDCl_3$): δ 1.29 (d, $^2J(H-P_A) = 8.4$, 3H, CH_3), 1.51 (s, 8H, CH_2 of COD), 3.32 (s, 4H, CH of COD), 5.53 (t, $^4J(H-P_B) = 4.2$, 1H, H$_4$), 6.67−8.05 (m, 30H, CH of Ph). ^{13}C ($CDCl_3$): δ 5.7 (s, $^1J(C-P_A) = 40.2$, CH_3), 32.9 (s, CH_2), 62.0 (d, $^2J(C-P_A) = 6.3$, CH of COD), 72.3 (dd, $^1J(C-P) = 95.9$, $^1J(C-P) = 39.3$, $C_{2,6}$), 117.1 (v q, $^4J(C-P_A) = {}^4J(C-P_B) = 10.7$, C_4H), 127.4−133.1 (m, CH of Ph), 134.4 (s, C of Ph), 135.7 (s, C of Ph), 143.3 (br s, $C_{3,5}$), 153.5 (br s, C of Ph).

Synthesis of Complex 7. A solution of MeLi in Et_2O (95 μL, $C = 1.6$ M, 0.15 mmol) was syringed into a solution of **1** (100 mg, 0.15 mmol) in THF (5 mL) at −78 °C. The solution was warmed to room temperature and stirred for 20 min. Complete formation of **2** is checked by ^{31}P NMR (THF): δ 44.83 (d, $^2J(P-P) = 156.7$, PPh_2), −66.52 (t, $^2J(P-P) = 156.7$, PMe). In the glovebox, [Ir(COE)$_2$Cl]$_2$ (63 mg, 0.8 mmol) and PPh$_3$ (40 mg, 15 mmol) were added, and the solution was stirred for 2 h. **7** was too sensitive to be dried or give satisfactory elemental data. Yield: 100%. ^{31}P (THF-d_8): δ 19.8 (td, $^2J(P_C-P_A) = 370.2$, $^2J(P_B-P_A) = 128.1$, P_AMe), 30.9 (td, $^2J(P_A-P_C) = 370.2$, $^3J(P_B-P_C) = 37.9$, P_CPh$_3$), 37.7 (dd, $^2J(P_B-P_A) = 128.1$, $^3J(P_B-P_C) = 37.9$, P_BPh$_2$).

Synthesis of Complex 8. A solution of MeLi in Et_2O (95 μL, $C = 1.6$ M, 0.15 mmol) was syringed into a solution of **1** (100 mg, 0.15 mmol) in THF (5 mL) at −78 °C. The solution was warmed to room temperature and stirred for 20 min. Complete formation of **2** is checked by ^{31}P NMR. In the glovebox, [Ir(COE)$_2$Cl]$_2$ (63 mg, 0.8 mmol) was added and the solution was stirred for 5 min. **8** decomposed within 30 min in THF; no NMR signal is then observed. ^{31}P (THF): δ 13.9 (t, $^2J(P_A-P_B) = 114.2$, P_AMe), 33.6 (d, $^2J(P_B-P_A) = 114.2$, P_BPh$_2$).

Synthesis of Complex 9. A solution of **5** (0.15 mmol) in THF (5 mL) was stirred under an O_2 atmosphere (1 atm) for 2 h, and an orange solid precipitated. The solid was filtered off and washed with THF (5 mL) and hexane (5 mL). **9** was recovered as an orange solid. Crystals of compound **9** suitable for X-ray diffraction deposited from a THF solution. Yield: 145 mg (82%). Anal. (%) Calcd for $C_{60}H_{49}IrO_2P_4S_2$: C 60.95, H 4.18. Found: C 60.53, H 3.91. ^{31}P (CD_2Cl_2): δ 4.9 (td, $^2J(P_C-P_A) = 428.5$, $^3J(P_C-P_B) = 24.2$, P_CPh$_3$), 17.7 (td, $^2J(P_A-P_C) = 428.5$, $^2J(P_A-P_B) = 100.1$, P_AMe), 50.2 (dd, $^2J(P_B-P_A) = 100.1$, $^3J(P_B-P_C) = 24.2$, P_BPh$_2$). ^1H (CD_2Cl_2): δ 1.32 (dd, $^2J(H-P) = 11.3$, $^4J(H-P) = 1.9$, 3H, CH_3), 5.77 (t, $^4J(H-P_B) = 4.4$, 1H, H$_4$), 6.87−8.07 (m, 45H, H of Ph). ^{13}C (CD_2Cl_2): δ 1.0 (m, CH_3), 69.5 (m, $C_{2,6}$), 116.2 (t, $^3J(C-P_B) = 11.8$, C_4), 126.4−133.8 (m, CH and C of Ph), 141.7 ($\Sigma J = 10.6$, $C_{3,5}$), 153.5 (bs, C of Ph).

Computational Details. Calculations were performed with the GAUSSIAN 03 series of programs[14] on the model systems [M(SPS)(PH$_3$)] and [M(SPS)(PH$_3$)(O$_2$)] (M = Rh, Ir) with the phenyl groups replaced by H atoms. Density functional theory (DFT)[15] was applied with the B3PW91 functional.[16] A quasirelativistic effective core potential operator was used to represent the 28 innermost electrons of the rhodium atom and the 60 innermost electrons of the iridium atom.[17] The basis set for the metal was that associated with the pseudopotential,[17] with a standard double-ζ LANL2DZ contraction[17] completed by a set of f-polarization functions.[18] The 6-31+G* basis set was used for O, P, and S atoms, 6-31G* for C atoms, and 6-31G for H atoms.[19] The minimum energy structures were characterized by full vibration frequencies calculations. The fully substituted square-planar complex [Rh(SPS)(PPh$_3$)] was

also optimized at the ONIOM(B3PW91/UFF) level,[20] where the QM part was treated within the framework of density functional theory at the B3PW91 and the UFF force field[21] was used for the molecular mechanics calculations (phenyl groups). In this QM/MM calculation, the basis set for the QM part is the same as that described above.

X-ray Crystallographic Study. A crystal of compound **10** suitable for X-ray diffraction deposited from a THF solution. Data were collected at 150.0(1) K on a Nonius Kappa CCD diffractometer using a Mo Kα ($\lambda = 0.71070$ Å) X-ray source and a graphite monochromator. All data were measured using phi and omega scans. Experimental details are described in Table 3. The crystal structures were solved using SIR 97[22] and SHELXL-97.[23] ORTEP drawings were made using ORTEP III for Windows.[24] CCDC-262573 contains the supplementary crystallographic data for this paper. These data can be obtained free of charge at www.ccdc.cam.ac.uk/conts/retrieving.html [or from the Cambridge Crystallographic Data Centre, 12 Union Road, Cambridge CB2 1EZ, UK; fax: (internat.) +44-1223/336-033; e-mail: deposit@ccdc.cam.ac.uk].

Supporting Information Available: Optimized geometry of [M(SPS)(PH$_3$)] (M = Rh, Ir) and **I−IV(a,b)**. This material is available free of charge via the Internet at http://pubs.acs.org.

OM049198C

(14) Frisch, M. J.; Trucks, G. W.; Schlegel, H. B.; Scuseria, G. E.; Robb, M. A.; Cheeseman, J. R.; J. A. Montgomery, J.; Vreven, T.; Kudin, K. N.; Burant, J. C.; Millam, J. M.; Iyengar, S. S.; Tomasi, J.; Barone, V.; Mennucci, B.; Cossi, M.; Scalmani, G.; Rega, N.; Petersson, G. A.; Nakatsuji, H.; Hada, M.; Ehara, M.; Toyota, K.; Fukuda, R.; Hasegawa, J.; Ishida, M.; Nakajima, T.; Honda, Y.; Kitao, O.; Nakai, H.; Klene, M.; Li, X.; Knox, J. E.; Hratchian, H. P.; Cross, J. B.; Adamo, C.; Jaramillo, J.; Gomperts, R.; Stratmann, R. E.; Yazyev, O.; Austin, A. J.; Cammi, R.; Pomelli, C.; Ochterski, J. W.; Ayala, P. Y.; Morokuma, K.; Voth, G. A.; Salvador, P.; Dannenberg, J. J.; Zakrzewski, V. G.; Dapprich, S.; Daniels, A. D.; Strain, M. C.; Farkas, O.; Malick, D. K.; Rabuck, A. D.; Raghavachari, K.; Foresman, J. B.; Ortiz, J. V.; Cui, Q.; Baboul, A. G.; Clifford, S.; Cioslowski, J.; Stefanov, B. B.; Liu, G.; Liashenko, A.; Piskorz, P.; Komaromi, I.; Martin, R. L.; Fox, D. J.; Keith, T.; Al-Laham, M. A.; Peng, C. Y.; Nanayakkara, A.; Challacombe, M.; Gill, P. M. W.; Johnson, B.; Chen, W.; Wong, M. W.; Gonzalez, C.; Pople, J. A. *GAUSSIAN 03*, Revision B.04; Gaussian, Inc.: Pittsburgh, PA, 2003.

(15) Parr, R. G.; Yang, W. *Density Functional Theory of Atoms and Molecules*; Oxford University Press: Oxford, U.K., 1989. Ziegler, T. *Chem. Rev.* **1991**, *91*, 651.

(16) Becke, A. D. *J. Chem. Phys.* **1993**, *98*, 5648.

(17) Hay, P. J.; Wadt, W. R. *J. Chem. Phys.* **1985**, *82*, 299.

(18) Ehlers, A.; Bohme, M.; Dapprich, S.; Gobbi, A.; Hollwarth, A.; Jonas, V.; Kohler, K.; Stegmenn, R.; Veldkamp, A.; Frenking, G. *Chem. Phys. Lett.* **1993**, *208*, 111.

(19) (a) Hehre, W. J.; Ditchfield, R.; Pople, J. A. *J. Chem. Phys.* **1972**, *56*, 2257. (b) Hariharan, P. C.; Pople, J. A. *Theor. Chim. Acta* **1973**, *28*, 213. (c) Francl, M. M.; Pietro, W. J.; Hehre, W. J.; Binkley, J. S.; Gordon, M. S.; DeFrees, D. J.; Pople, J. A. *J. Chem. Phys.* **1982**, 77, 3654. (d) Clark, T.; Chandrasekhar, J.; Spitznagel, G. W.; Schleyer, P. v. R. *J. Comput. Chem.* **1983**, *4*, 294.

(20) Svensson, M.; Humbel, S.; Froese, R. D. J.; Matsubara, T.; Sieber, S.; Morokuma, K. J. *J. Phys. Chem.* **1996**, *100*, 19357.

(21) Rappé, A. K.; Casewitt, C. J.; Colwell, K. S.; Goddard, W. A.; Skiff, W. M. *J. Am. Chem. Soc.* **1992**, *114*, 10024.

(22) Altomare, A.; Burla, M. C.; Camalli, M.; Cascarano, G.; Giacovazzo, C.; Guagliardi, A.; Moliterni, A. G. G.; Polidori, G.; Spagna, R. *SIR97, an integrated package of computer programs for the solution and refinement of crystal structures using single-crystal data;* Institute of Crystallography, Bari, Italy, 1988.

(23) Sheldrick, G. M. *SHELXL-97*; Universität Göttingen: Göttingen, Germany, 1997.

(24) Farrugia, L. J. *ORTEP-3*; Department of Chemistry, University of Glasgow, Glasgow, Scotland, 2003.